ÎMBUNĂTĂȚIREA CARACTERISTICILOR MECANICE ALE STRATIFICATELOR COMPOZITE PRIN ALEGEREA RAȚIONALĂ A MATERIALELOR ȘI CONFIGURAȚIILOR CORESPUNZĂTOARE

IMPROVING THE MECHANICAL PROPERTIES OF COMPOSITE LAMINATES THROUGH THE SUITABLE SELECTION OF THE CORRESPONDING MATERIALS AND CONFIGURATIONS

IULIANA HUDIȘTEANU, NICOLAE ȚĂRANU*, DORINA NICOLINA ISOPESCU, LILIANA BEJAN, ANDREI AXINTE, DRAGOȘ UNGUREANU

"Gheorghe Asachi" Technical University of Iaşi, 1 Mangeron Blvd., Iaşi, Romania, 700050

The paper presents a comparative analysis of six cases of symmetrically balanced composite laminates, having the same stacking sequences in terms of fibre orientation angles, but different composite laminas. The purpose of the paper is to investigate the influence of the selection of the composite materials and configurations of the laminas on the mechanical performances of laminated composites.

A finite element analysis in ANSYS Composite Pre/Post software is performed in order to study the mechanical characteristics under tensile loading of the composite laminates and to analyse the stresses and damage distributions on each layer with different fibre orientations.

The results are comparatively presented in terms of the in-plane and flexural engineering constants of the considered laminates, ultimate loads when first ply failure (FPF) and last ply failure (LPF) occur, and their corresponding equivalent stresses on the layers of the laminates.

The damage initiation and damage evolution on the layers of the composite elements are indicated for different loading steps.

Lucrarea prezintă o analiză comparativă realizată pe 6 cazuri de stratificate compozite simetrice echilibrate, având aceeași ordine de succesiune a lamelelor din punctul de vedere al orientării fibrelor, dar alcătuite din materiale compozite diferite. Obiectivul lucrării este de a investiga influența selectării materialelor compozite și a configurațiilor corespunzătoare ale lamelelor, asupra performanțelor mecanice ale stratificatelor compozite.

O analiză bazată pe metoda elementelor finite este realizată în programul de calcul ANSYS Composite Pre/Post, pentru a studia comportamentul mecanic al stratificatelor echilibrate solicitate la întindere și a urmări distribuția tensiunilor și degradărilor pe fiecare strat cu orientare diferită a fibrelor.

Rezultatele sunt prezentate comparativ pentru constantele elastice inginerești în planul stratificatelor și la încovoiere, pentru forțele de cedare ale primei și ultimei lamele din cadrul fiecărui stratificat, precum și a tensiunilor echivalente pe straturile elementare corespunzătoare forțelor ultime determinate. Inițierea și evoluția degradărilor pe straturile elementelor stratificate sunt localizate pentru diferite trepte de încărcare.

Keywords: *composite laminates, failure criteria, first ply failure, last ply failure, damage initiation and evolution*

1. Introduction

The composite laminates can be defined as multi-layered elements made of two or more composite laminas stacked together, having the same or different fibre orientation angles, materials constituents and thicknesses [1]. The most important challenge of conceiving and designing laminated composites is the prediction of their mechanical properties [2].

A complex study is carried out in order to evaluate the possibility of improving the stiffness and strength properties of the composite laminates, by choosing the corresponding composite materials and configurations. The analysed multi-layered composites are balanced laminates, with fibre orientation angles selected such that a progressive damage occurs and a catastrophic failure is prevented.

The study involves an extensive numerical analysis, using finite element method in ANSYS Composite Pre/Post software, performed in order to characterise the mechanical behaviour of the multi-layered composites under tensile loading.

A progressive damage analysis is carried out, associated with the damage appearance and evolution in the composite material and the local failures of the laminas.

Progressive damage is defined based on the damage initiation criteria and damage evolution law [3]. Damage initiation criteria refers to the failure criteria adopted to evaluate the material damage under loading. The damage evolution law establishes, based on a stiffness reduction coefficient, the way in which the material degrades after the initiation of damage occurs.

The progressive damage of composite laminates is still an actual concern [4, 5].

* Autor corespondent/*Corresponding author*,
E-mail: taranu@ce.tuiasi.ro

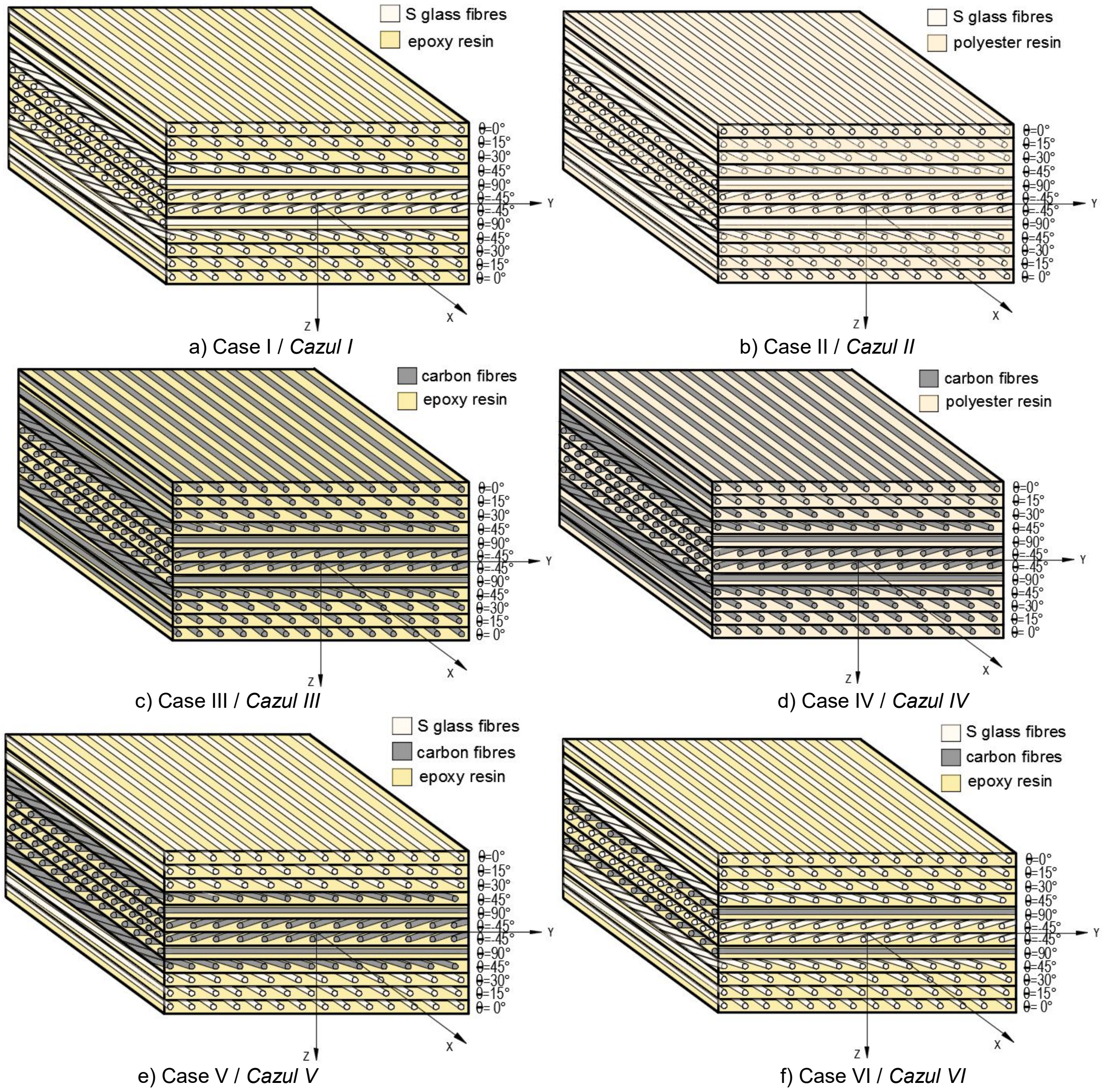

a) Case I / *Cazul I* b) Case II / *Cazul II*

c) Case III / *Cazul III* d) Case IV / *Cazul IV*

e) Case V / *Cazul V* f) Case VI / *Cazul VI*

Fig. 1 - 3D configurations of the analysed laminated composites / *Configurațiile 3D ale stratificatelor compozite analizate.*

2. Case study configurations

Six stacking sequences of symmetrically balanced composite laminates are analysed, having the configurations $[0/15/30/45/90/-45]_s$, illustrated in Figure 1. For the case study, the composite laminates are made of 12 layers, with a total thickness of 3 mm, as to ensure the stiffness of the plates.

Two types of continuous fibres and two thermosetting resins have been selected as constituents for the composite material, such as: S glass and high stiffness carbon fibres, and epoxy and polyester resin. The first four cases of laminates are made of one type composite material laminas, such as: *Case I* – S glass fibres and epoxy resin; *Case II* – S glass fibres and polyester resin; *Case III* – carbon fibres and epoxy resin; *Case IV* – carbon fibres and polyester resin.

The S glass fibres provide higher strength properties at low costs, while the carbon fibres have higher stiffness characteristics in the fibre direction, but they are more expensive [6-9]. An improved solution in terms of mechanical performances and costs can be considered by conceiving hybrid composite laminates [10, 11]. Therefore, the *Case V* and *Case VI* are built-up starting from the *Case I* laminate, composed in such a way that the layers with poor stiffness properties, having the fibre orientation angles of ±45° and 90°, are replaced with laminas made of carbon fibres and epoxy resin. The first hybrid laminate (*Case V*) has 6 layers made of S glass fibres and epoxy resin and 6 layers of carbon fibres and epoxy matrix, while the *Case VI* hybrid laminate has only the laminas reinforced with carbon fibres having the fibre orientation angles at 90°.

Each layer of the laminates has the same fibre volume fraction V_f = 60%, the lamina thickness is 0.25 mm and the in-plane dimensions of the composite plate are 500 mm x 500 mm. The

Table 1

Material consumption and cost of the laminates / *Cantitățile de materiale și costul stratificatelelor [12]*

The analysed cases of composite laminates *Stratificatele compozite analizate*		The constituent material's density *Densitatea materialelor constituente* [kg/m³]	Material consumption *Consumul de materiale* [kg]	Price/kg *Preț/kg* [EUR/kg]	Total price *Preț total* [EUR]
Case I	S glass fibres / *fibre de sticlă S*	2500	1.125	3	118.65
	epoxy resin / *rășină epoxidică*	1400	0.42	2.5	
Case II	S glass fibres / *fibre de sticlă S*	2500	1.125	3	115.10
	polyester resin / *rășină poliesterică*	1250	0.375	2	
Case III	carbon fibres / *fibre de carbon*	1950	0.878	30	460.21
	epoxy resin / *rășină epoxidică*	1400	0.42	2.5	
Case IV	carbon fibres / *fibre de carbon*	1950	0.878	30	459.22
	polyester resin / *rășină poliesterică*	1250	0.375	2	
Case V	S glass fibres / *fibre de sticlă S*	2500	0.563	3	246.52
	carbon fibres / *fibre de carbon*	1950	0.439	30	
	epoxy resin / *rășină epoxidică*	1400	0.42	2.5	
Case VI	S glass fibres / *fibre de sticlă S*	2500	0.938	3	145.55
	carbon fibres / *fibre de carbon*	1950	0.146	30	
	epoxy resin / *rășină epoxidică*	1400	0.42	2.5	

Table 2

Mechanical properties of constituent materials / *Caracteristicile mecanice ale materialelor constituente [13]*

Constituents of the composite laminas *Materialele constituente ale lamelelor compozite*	Fibres / Fibre		Matrix / Matrice	
	S glass *sticlă S*	carbon *carbon*	epoxy *epoxidică*	polyester *poliesterică*
Elastic modulus *Modulul de elasticitate* **E_f / E_m** [GPa]	85.5	E_{fl} *= 380 E_{ft} **= 6.2	4.1	4
Poisson's ratio *Coeficientul lui Poisson* **υ_f / υ_m**	0.22	0.20	0.40	0.39
Longitudinal tensile strength *Rezistența la tracţiune longitudinală* **f_{ft} / f_{mt}** [MPa]	4580	2100	75	70
Longitudinal compressive strength *Rezistența la compresiune longitudinală* **f_{fc} / f_{mc}** [MPa]	2450	1500	150	120
In-plane shear strength *Rezistența la forfecare în planul LT* **f_{fs} / f_{ms}** [MPa]	-	-	70	60
The ultimate specific strain at longitudinal traction *Deformația specifică ultimă la tracţiune longitudinală* **ε_{fu} / ε_{mu}** [%]	5	0.5	6.2	5.1

* elastic modulus of the carbon fibres in the longitudinal direction;
** elastic modulus of the carbon fibres in the transverse direction.

material consumption is presented in Table 1. The total prices of laminates given in Table 1 take into account only the constituents' materials cost, since they are the only variable parameters. The cost of manufacturing, by hand lay-up, is assumed to be the same for every case.

3. Micromechanical properties of the composite laminas

The properties of the constituents utilised in evaluation of the mechanical characteristics of the analysed composite laminas, based on micromechanics, are given in Table 2.

The stiffness properties of the composite laminas, determined by micromechanical analysis, are: E_1 – the elastic modulus in the fibre direction; E_2 – the elastic modulus in the direction normal to the fibre direction; G_{12} – the in-plane shear modulus; G_{23} – the out-of-plane shear modulus; υ_{12} – the in-plane major Poisson's ratio.

The strength parameters of the composite lamina are: f_{1t} – the longitudinal tensile strength; f_{1c} – the longitudinal compressive strength; f_{2t} – the transverse tensile strength; f_{2c} – the transverse compressive strength; f_{12s} – the in-plane shear strength and f_{23s} – the intralaminar shear strength.

The micromechanical properties of the laminas are evaluated according to the relations presented below, for each corresponding composite material, in order to be used as input data in the numerical analysis in ANSYS software.

The relations for determining the micromechanical characteristics of the composite laminas are selected from Barbero [14], taking into account the orthotropic behaviour of the carbon fibres.

The longitudinal modulus of the composite laminas is computed with *the rule of mixture*:

$$E_1 = E_{fl}V_f + E_m(1 - V_f) \quad (1)$$

The transverse modulus of the composite laminas with isotropic fibres is computed according to *the stress partitioning method*, as follows [14]:

$$E_2 = E_m \frac{V_f + \eta_2 (1 - V_f)}{\eta_2 (1 - V_f) + V_f E_m / E_f}, \quad (2a)$$

where $\eta_2 = \frac{1}{2}\left(1 + \frac{E_m}{E_f}\right)$ (2b)

In case of the composite laminas reinforced with carbon fibres, *the transverse modulus* of the composite laminas is computed according to *the Halpin-Tsai* relation [15]:

$$E_2 = E_m \frac{1 + \zeta \eta V_f}{1 - \eta V_f}, \quad (3a)$$

where $\eta = \frac{E_{ft} / E_m - 1}{E_{ft} / E_m + \zeta}$, $\zeta = 2$ (3b)

ζ represents the reinforcing efficiency factor for transverse loading [15].

The in-plane shear modulus of the composite laminas is evaluated with *the cylindrical assemblage model* [12]:

$$G_{12} = G_m \frac{(1 + V_f) + (1 - V_f) G_m / G_f}{(1 - V_f) + (1 + V_f) G_m / G_f}, \quad (4a)$$

where $G_f = \frac{E_f}{2(1 + \nu_f)}$ and $G_m = \frac{E_m}{2(1 + \nu_m)}$ are the shear moduli of the constituents. (4b)

The intralaminar shear modulus of the composite laminas is computed according to the *stress partitioning method*, as follows [14]:

$$G_{23} = G_m \frac{V_f + \eta_4 (1 - V_f)}{\eta_4 (1 - V_f) + V_f G_m / G_f}, \quad (5a)$$

where $\eta_4 = \frac{3 - 4\nu_m + G_m / G_f}{4(1 - \nu_m)}$ (5b)

The in-plane Poisson's ratio is determined according to *the rule of mixture*:

$$\nu_{12} = \nu_f V_f + \nu_m (1 - V_f) \quad (6)$$

The longitudinal tensile strength is evaluated with the following relation [16]:

$$f_{1t} = f_{ft}\left[V_f + \frac{E_m}{E_f}(1 - V_f)\right] \quad (7)$$

Table 3

Mechanical properties of unidirectional fibre reinforced laminas / *Caracteristicile mecanice ale lamelelor compozite armate cu fibre unidirecționale*

Mechanical properties of composite laminas / *Proprietățile mecanice ale lamelelor compozite*		Fibres / *Fibre*	S glass / *sticlă S*	S glass / *sticlă S*	carbon / *carbon*	carbon / *carbon*
		Matrix / *Matrice*	epoxy / *epoxidică*	polyester / *poliesterică*	epoxy / *epoxidică*	polyester / *poliesterică*
Stiffness properties of the laminas / *Caracteristici elastice ale lamelelor*	Longitudinal modulus / *Modulul de elasticitate longitudinal* **E1** [GPa]		52.94	52.90	229.60	229.60
	Transverse modulus / *Modulul de elasticitate transversal* **E2** [GPa]		13.93	13.64	5.28	5.23
	In-plane shear modulus / *Modulul de elasticitate la forfecare în planul lamelei* **G12** [GPa]		5.07	4.99	5.66	5.56
	Out-of-plane shear modulus / *Modulul de elasticitate la forfecare perpendicular pe planul lamelei* **G23** [GPa]		4.63	4.53	5.08	4.96
	In-plane Poisson's ratio / *Coeficientul lui Poisson în planul (12)* ν_{12}		0.292	0.288	0.28	0.276
	Out-of-plane Poisson's ratio / *Coeficientul lui Poisson în planul (23)* ν_{23}		0.554	0.539	0.575	0.557
Strength properties of the laminas / *Caracteristici de rezistență ale lamelelor*	Longitudinal tensile strength / *Rezistența la tracțiune longitudinală* **f1t** [MPa]		2836	2834	1269	1269
	Longitudinal compressive strength / *Rezistența la compresiune longitudinală* **f1c** [MPa]		1122	1014	1166	1052
	Transverse tensile strength / *Rezistența la tracțiune transversală* **f2t** [MPa]		62.53	58.35	70.56	65.66
	Transverse compressive strength / *Rezisțența la compresiune transversală* **f2c** [MPa]		125.1	100	141.1	112.6
	In-plane shear strength / *Rezistența la forfecare în planul (12)* **f12f** [MPa]		58.29	49.95	57.89	49.62
	Out-of-plane shear strength / *Rezistența la forfecare în planul (23)* **f23f** [MPa]		45.43	36.34	51.27	40.89

The longitudinal compressive strength is determined according to Eq. (8), as follows [14]:

$$f_{1c} = G_{12}(1+4.76\chi)^{-0.69}, \qquad (8a)$$

where $$\chi = \frac{G_{12}\cdot\alpha_\sigma}{f_{12s}}, \alpha_\sigma = 1.1, \qquad (8b)$$

α_σ - standard deviation of fiber misalignement.

The transverse tensile strength is computed according to [14]:

$f_{2t} = f_{mt}C_v\left[1+\left(V_f-\sqrt{V_f}\right)\left(1-\frac{E_m}{E_{ft}}\right)\right]$, where C_v = void reduction coefficient =1, for no voids. (9)

The transverse compressive strength is determined according to Eq. (10), [14]:

$$f_{2c} = f_{mc}C_v\left[1+\left(V_f-\sqrt{V_f}\right)\left(1-\frac{E_m}{E_{ft}}\right)\right] \qquad (10)$$

The in-plane shear strength is computed according to [14]:

$$f_{12s} = f_{ms}C_v\left[1+\left(V_f-\sqrt{V_f}\right)\left(1-\frac{G_m}{G_f}\right)\right] \qquad (11)$$

The intralaminar shear strength is determined according to Eq. (12):

$f_{23s} = f_{2c}\cdot\cos\alpha_0(\sin\alpha_0+\cos\alpha_0\cdot c\tan 2\alpha_0)$,

where $\alpha_0 = 54°$ - fiber misalignment [14]. (12)

The stiffness and strength properties obtained using the Eq. (1) – (12) are centralised in Table 3, for each analysed lamina.

4. Stiffness properties of the composite laminates

4.1. Evaluation of the in-plane and flexural engineering constants

The constitutive relation of composite laminates is written for an elementary layer *k* of a generally orthotropic lamina, given by Eq. (13a) and (13b) [14]:

$$\begin{Bmatrix}\sigma_x\\ \sigma_y\\ \tau_{xy}\end{Bmatrix}_k = \begin{bmatrix}\overline{Q}_{11} & \overline{Q}_{12} & \overline{Q}_{16}\\ \overline{Q}_{12} & \overline{Q}_{22} & \overline{Q}_{26}\\ \overline{Q}_{16} & \overline{Q}_{26} & \overline{Q}_{66}\end{bmatrix}_k \begin{Bmatrix}\varepsilon_x\\ \varepsilon_y\\ \gamma_{xy}\end{Bmatrix}_k \qquad (13a)$$

$$\begin{Bmatrix}\tau_{yz}\\ \tau_{xz}\end{Bmatrix}_k = \begin{bmatrix}\overline{Q}^*_{44} & \overline{Q}^*_{45}\\ \overline{Q}^*_{45} & \overline{Q}^*_{55}\end{bmatrix}_k \begin{Bmatrix}\gamma_{yz}\\ \gamma_{xz}\end{Bmatrix}_k \qquad (13b)$$

where: (σ_x, σ_y, τ_{xy}) are the in-plane stress components in the global reference system of axes; (ε_x, ε_y, γ_{xy}) are the in-plane strain components in the global reference system of axes; (τ_{yz}, τ_{xz}) represent the intralaminar shear stresses along the global reference axes; (γ_{yz}, γ_{xz}) represent the intralaminar shear strains along the global reference axes;

$\left[\overline{Q}\right]$ is the transformed reduced stiffness matrix;

$\left[\overline{Q}^*\right]$ is the transformed intralaminar stiffness matrix.

The force-deformation and moment-deformation expressions of multi-layered laminates are described by Eq. (14), as well as their inverse forms in Eq. (15), as follow:

$$\begin{Bmatrix}N_x\\ N_y\\ N_{xy}\end{Bmatrix} = \begin{bmatrix}A_{11} & A_{12} & A_{16}\\ A_{12} & A_{22} & A_{26}\\ A_{16} & A_{26} & A_{66}\end{bmatrix}\begin{Bmatrix}\varepsilon_x^0\\ \varepsilon_y^0\\ \gamma_{xy}^0\end{Bmatrix}, \qquad (14a)$$

$$\begin{Bmatrix}V_x\\ V_y\end{Bmatrix} = \begin{bmatrix}C_{44} & C_{45}\\ C_{54} & C_{55}\end{bmatrix}\begin{Bmatrix}\gamma_{yz}\\ \gamma_{zx}\end{Bmatrix}, \qquad (14b)$$

$$\begin{Bmatrix}M_x\\ M_y\\ M_{xy}\end{Bmatrix} = \begin{bmatrix}D_{11} & D_{12} & D_{16}\\ D_{12} & D_{22} & D_{26}\\ D_{16} & D_{26} & D_{66}\end{bmatrix}\begin{Bmatrix}k_x\\ k_y\\ k_{xy}\end{Bmatrix}, \qquad (14c)$$

$$\begin{pmatrix}\varepsilon_x^0\\ \varepsilon_y^0\\ \gamma_{xy}^0\end{pmatrix} = \begin{bmatrix}A'_{11} & A'_{12} & A'_{16}\\ A'_{12} & A'_{22} & A'_{26}\\ A'_{16} & A'_{26} & A'_{66}\end{bmatrix}\begin{pmatrix}N_x\\ N_y\\ N_{xy}\end{pmatrix} \qquad (15a)$$

$$\begin{Bmatrix}\gamma_{yz}\\ \gamma_{zx}\end{Bmatrix} = \begin{bmatrix}C'_{44} & C'_{45}\\ C'_{54} & C'_{55}\end{bmatrix}\begin{Bmatrix}V_x\\ V_y\end{Bmatrix} \qquad (15b)$$

$$\begin{pmatrix}k_x\\ k_y\\ k_{xy}\end{pmatrix} = \begin{bmatrix}D'_{11} & D'_{12} & D'_{16}\\ D'_{12} & D'_{22} & D'_{26}\\ D'_{16} & D'_{26} & D'_{66}\end{bmatrix}\begin{pmatrix}M_x\\ M_y\\ M_{xy}\end{pmatrix} \qquad (15c)$$

where:

(N_x, N_y, N_{xy}), (M_x, M_y, M_{xy}) are the resultant in-plane forces and moments per unit length;

(V_x, V_y) are the resultant intralaminar shear forces per unit length;

(ε_x^0, ε_y^0, γ_{xy}^0) represents the laminate mid-plane strains;

(k_x, k_y, k_{xy}) represents the laminate curvatures;

(γ_{yz}, γ_{xz}) represent the intralaminar shear strains.

$[A]$ is the in-plane stiffness matrix, $[D]$ is the bending stiffness matrix and $[C]$ is the transverse shear stiffness matrix.

The elastic engineering constants of multi-layered composites are: E_x – the in-plane longitudinal modulus, E_y – the in-plane transverse modulus, G_{xy} – the in-plane shear modulus, E_x^f – the flexural longitudinal modulus, E_y^f – the flexural transverse modulus, G_{xy}^f – the flexural shear modulus, G_{yz} and G_{zx} the out-of-plane (intralaminar) shear moduli.

The relations used to evaluate the engineering constants for the symmetrically balanced composite laminate are given by Eq. (16), as follows [14, 17, 18]:

$$E_x = \frac{1}{2H \cdot A'_{11}},\ E_y = \frac{1}{2H \cdot A'_{22}},\ G_{xy} = \frac{1}{2H \cdot A'_{66}}$$
$$E^f_x = \frac{12}{(2H)^3 \cdot D'_{11}},\ E^f_y = \frac{12}{(2H)^3 \cdot D'_{22}},\ G^f_{xy} = \frac{12}{(2H)^3 \cdot D'_{66}} \qquad (16)$$
$$G_{yz} = \frac{1}{2H \cdot C'_{44}} \cdot k_{44},\ G_{zx} = \frac{1}{2H \cdot C'_{55}} \cdot k_{55},$$

where: 2H is the total thickness of the laminate, k_{44} and k_{55} are the shear correction factors, provided by [3].

4.2. Results and discussions

The in-plane and flexural engineering constants, as well as the interlaminar shear moduli are comparatively presented in Figure 2, for each analysed case of multi-layered composites.

The laminates made of epoxy matrix have properties very close to those made of polyester resin, for the same type of embedded fibres. Significant differences are noticed between the S glass fibre type laminates and those made of carbon fibres. The in-plane and flexural longitudinal properties of the studied configuration of balanced laminates reinforced with carbon fibres are approximately 3 times higher than those reinforced with S glass fibres. Although the carbon fibres' orthotropy is considered, the transverse stiffness properties of *Case III* and *Case IV* are more than 2 times greater than the first 2 cases of multi-layered composites; this characteristic is valid only for the in-plane behaviour.

The in-plane shear stiffness is 3 times greater for carbon fibre types laminates than the S glass fibre multi-layered composites, while the out-of-plane shear moduli are approximately 1.5 times greater in case of S glass fibres laminates compared to those made only of carbon fibres.

The hybrid laminates offer improved elastic results in case of in-plane and flexural transverse and shear moduli. Therefore, they could be considered as solutions when enhanced stiffness properties are needed in these directions.

The polar plots of the in-plane elastic engineering constants of the balanced laminates, rotated from 0° to 360°, are illustrated in Figure 3. Due to the similarity of the *Case I* with *Case II* and of the *Case III* with *Case IV*, only the laminates made of epoxy resin are shown in the representation. The variation of engineering constants in polar coordinates can be considered as an envelope of the elastic safety behaviour. The representation of the stiffness properties in polar coordinates indicates the influence of the orientation and the anisotropy of the composite laminates.

Comparing the polar distributions of the represented cases, the hybrid I laminate (*Case V*) has the most balanced elastic properties with respect to the orientation and the largest envelope of elastic safety behaviour.

The in-plane engineering constants represented in Figure 2, are also given in polar coordinates in Figure 3, corresponding to the angle of 0°.

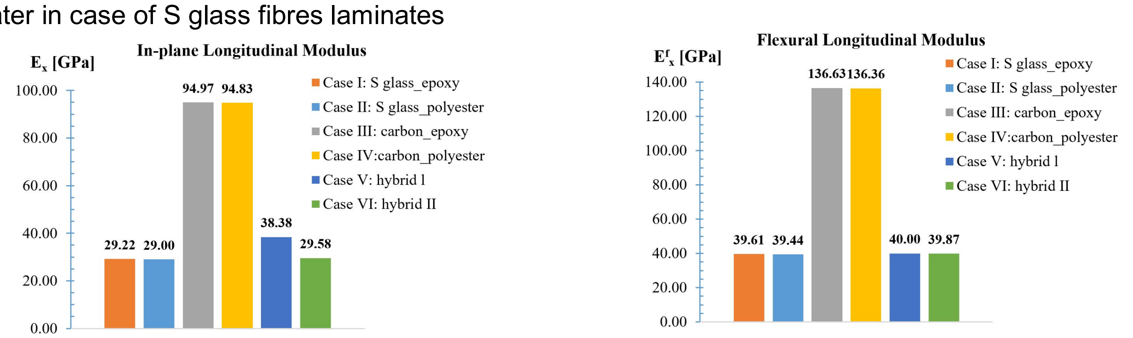

a) The in-plane and flexural longitudinal moduli / *Modulii de elasticitate longitudinali în plan și la încovoiere*

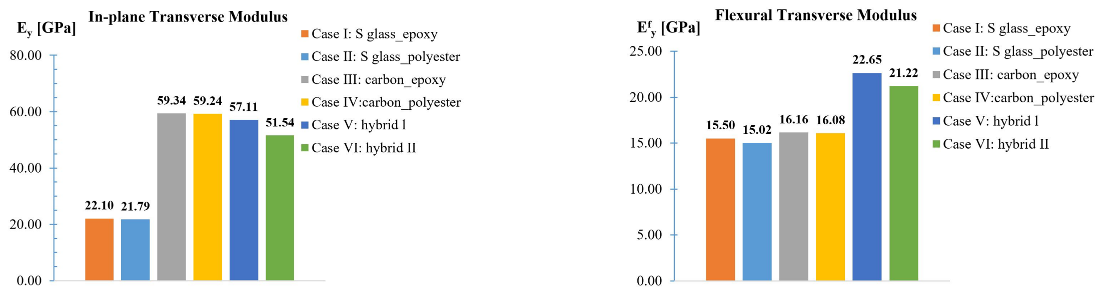

b) The in-plane and flexural transverse moduli / *Modulii de elasticitate transversali în plan și la încovoiere*

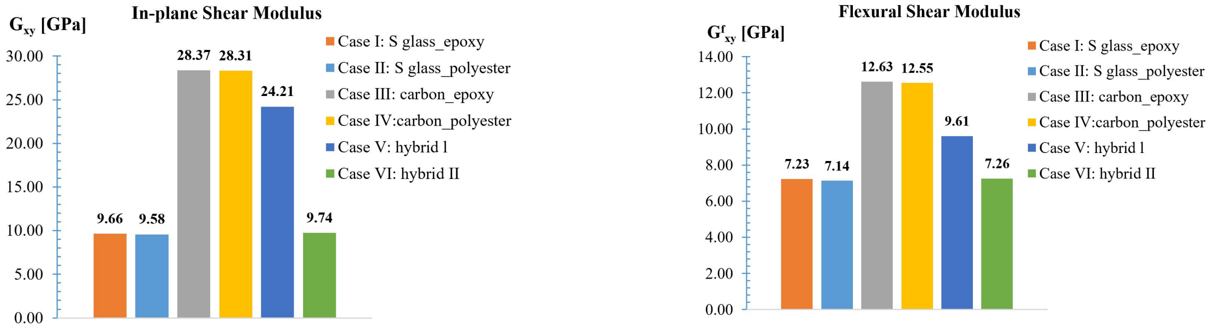

c) The in-plane and flexural shear moduli / *Modulii de elasticitate la forfecare în plan și la încovoiere*

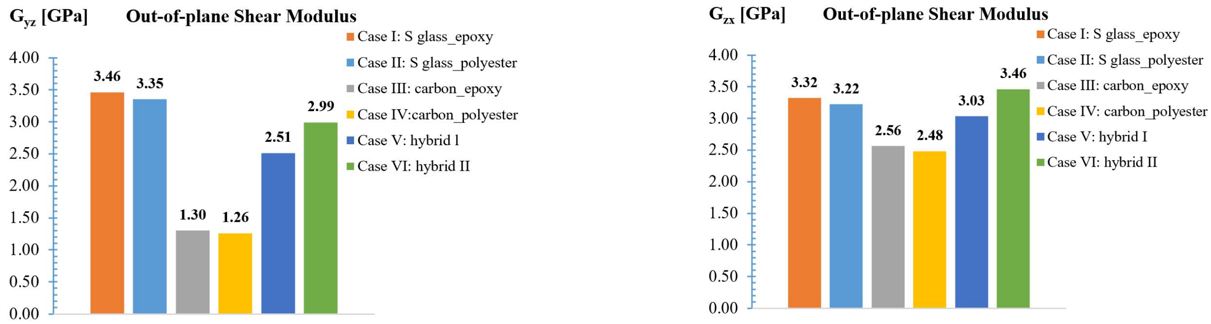

d) The out-of-plane shear moduli / *Modulii de elasticitate la forfecare intralamelară*

Fig. 2 - The elastic engineering constants for balanced laminates / *Constante elastice inginerești ale stratificatelor echilibrate.*

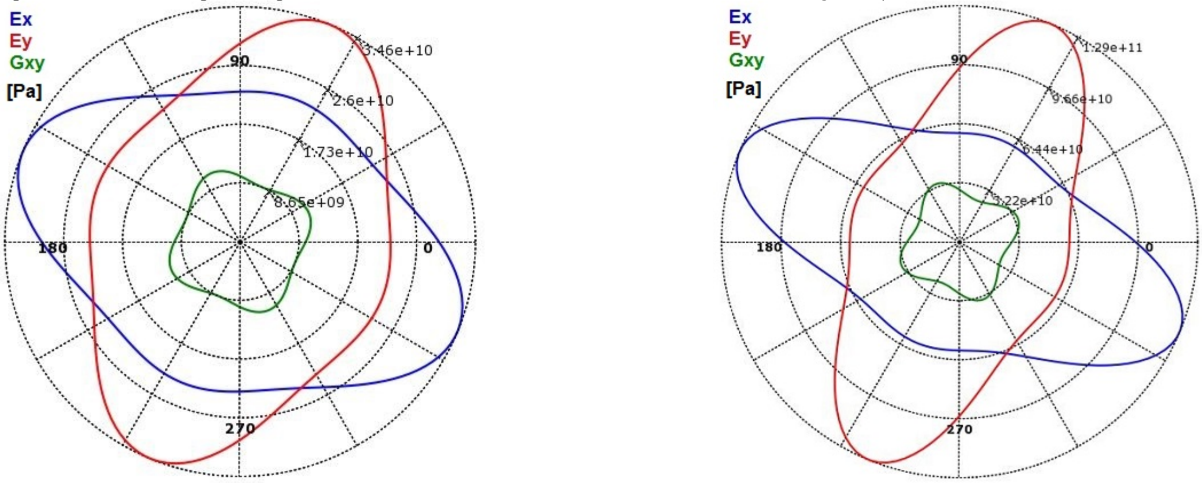

a) Case I / *Cazul I*

b) Case III/ *Cazul III*

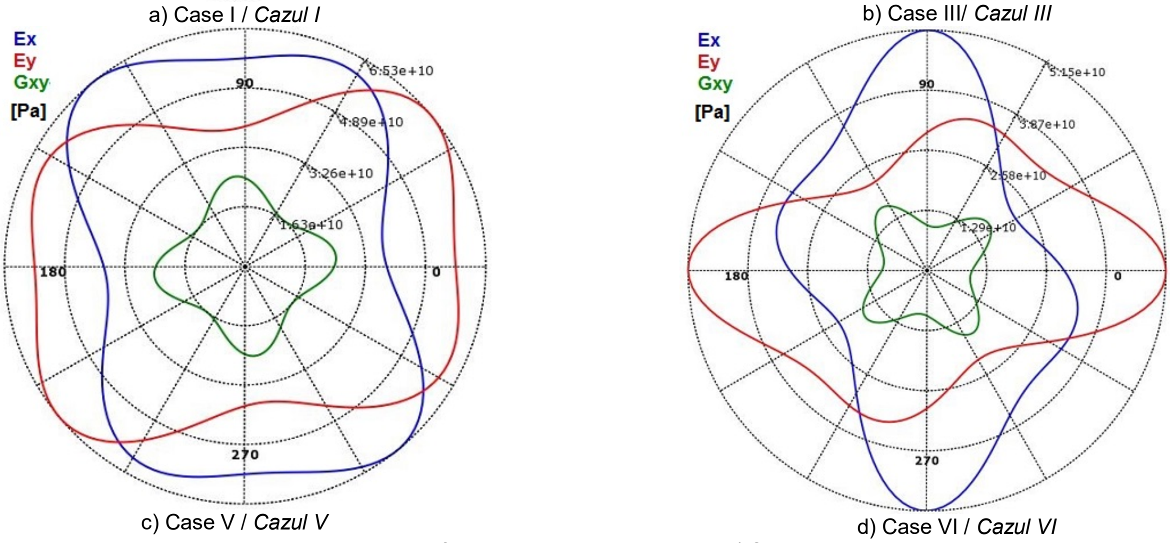

c) Case V / *Cazul V*

d) Case VI / *Cazul VI*

Fig. 3 - Engineering constants in polar coordinates for composite laminated cases / *Constante inginerești în coordonate polare ale stratificatelor compozite analizate.*

5. Comparative strength performances of the analysed composite laminates

To perform a progressive failure analysis for predicting the strength characteristics under tensile loading on x direction of the multi-layered composites, the maximum strain failure criterion has been selected in the numerical modelling.

5.1. Maximum strain failure criterion

According to the maximum strain failure criterion, the failure occurs when any component of the specific strain on the principal material axes exceeds the corresponding ultimate specific strain [1, 8]:

$$-\varepsilon_{1c} < \varepsilon_1 < \varepsilon_{1t}$$
$$-\varepsilon_{2c} < \varepsilon_2 < \varepsilon_{2t} \qquad (17)$$
$$-\gamma_{12f} < \gamma_{12} < \gamma_{12f}$$

where:

ε_{1t}, ε_{2t} - the ultimate tensile strains in the longitudinal and transverse direction, respectively;

ε_{1c}, ε_{2c} - the ultimate compressive strains in the longitudinal and transverse direction, respectively;

γ_{12f} - the ultimate in-plane shear strain.

The effective strains with respect to the material axes $(\varepsilon_1, \varepsilon_2, \gamma_{12})$, for a loading action equivalent with σ_x, are determined with the following relations:

$$\varepsilon_1 = \frac{\sigma_x}{E_1}\left(\cos^2\theta - \nu_{12}\sin^2\theta\right)$$
$$\varepsilon_2 = \frac{\sigma_x}{E_2}\left(\sin^2\theta - \nu_{21}\cos^2\theta\right) \qquad (18)$$
$$\gamma_{12} = \frac{\sigma_x}{G_{12}}\sin\theta\cos\theta .$$

5.2. Results and discussions

The results are presented in Table 4, in terms of ultimate loads at FPF and the corresponding equivalent stresses on each layer of the laminate. Moreover, the ultimate loads for LPF are determined.

Table 4

Mechanical properties of the laminates analysed cases / *Caracteristicile mecanice ale stratificatelor analizate*

Cases / *Cazuri*	Results on ply sets *Rezultate pe straturi*	Ultimate load FPF *Forța ultimă* CPL* [kN]	Equiv. stress *Tensiuni echivalente* σ_{ech} [MPa]	Shear stress *Tensiuni tangențiale* τ [MPa]	Strain energy *Energia potențială de deformație* [mJ]	Elongation *Alungirea* [mm]	Failure index *Indicele de cedare*	Ultimate load LPF *Forța ultimă* CUL** [kN]	Equiv. stress *Tensiuni echivalente* σ_{ech} [MPa]
Case I / *Cazul I*	1 (0°)	118.660 (ply 5)	255.86	6.29	89.024	1.35	0.31	373.897 (ply 1)	**806.24**
	2 (15°)		232.98	48.32			0.49		734.11
	3 (30°)		194.56	67.84			0.54		613.07
	4 (45°)		136.44	54.47			0.84		429.93
	5 (90°)		**106.34**	6.29			1		335.08
	6 (-45°)		220.7	-10.67			0.51		695.43
Case II / *Cazul II*	1 (0°)	115.090 (ply 5)	248.93	5.84	83.61	1.32	0.35	324 (ply 1)	**700.93**
	2 (15°)		226.13	46.91			0.55		636.66
	3 (30°)		188.32	65.89			0.60		530.14
	4 (45°)		131.49	52.86			0.84		370.06
	5 (90°)		**101.42**	5.84			1		285.69
	6 (-45°)		214.66	-11.38			0.53		604.55
Case III / *Cazul III*	1 (0°)	460.210 (ply 1)	**1330.9**	4.38	416.39	1.63	1	847.695 (ply 5)	2449.60
	2 (15°)		1107.2	260.73			0.81		2038.60
	3 (30°)		858.59	354.28			0.79		1580.5
	4 (45°)		529.06	258.74			0.66		975.34
	5 (90°)		435.98	4.38			0.54		**803.44**
	6 (-45°)		1283.9	-133.42			0.94		2364.60
Case IV / *Cazul IV*	1 (0°)	459.225 (ply 1)	**1328.9**	4.31	415.87	1.63	1	735.90 (ply 5)	2130.8
	2 (15°)		1106.6	260.86			0.88		1772.4
	3 (30°)		857.85	354.28			0.90		1373.6
	4 (45°)		528.25	258.45			0.76		847.05
	5 (90°)		436.95	4.31			0.62		**700.54**
	6 (-45°)		1285.3	-133.22			0.95		2058.6
Case V / *Cazul V*	1 (0°)	246.517 (ply 6)	431.04	11.86	349.91	2.11	0.35	696 (ply 1)	**1217.20**
	2 (15°)		412.17	88.65			0.68		1164.20
	3 (30°)		351.77	125.75			0.82		993.52
	4 (45°)		1076.6	531.32			0.90		3037.30
	5 (90°)		556.79	13.28			0.58		1571.10
	6 (-45°)		**1352.9**	-114.87			1		3822.8
Case VI / *Cazul VI*	1 (0°)	175.547 (ply 4)	306.32	3.56	132.08	1.98	0.33	526 (ply 1)	**917.83**
	2 (15°)		272.46	53.17			0.54		816.40
	3 (30°)		222.14	74.23			0.62		665.60
	4 (45°)		**153.52**	57.88			1		460.01
	5 (90°)		200.05	3.98			0.41		599.36
	6 (-45°)		255.13	-30.31			0.58		764.47

*CPL – cedarea primei lamele; **CUL – cedarea ultimei lamele.

The results are given in Table 4, for 6 layers of each of the cases. The ultimate load at FPF for *Case III* and *IV* is almost 4 times greater than in the case of S glass fibre type laminates. Improved strength properties are noticed also for the considered hybrid laminates.

Although the composite laminates have the same fibre orientation configurations, the plies failure sequence is different in every case, meaning that the influence of the adopted composite material is significant.

The equivalent stresses distributions on the layers of the *Case I* composite laminate are shown in Figure 4, for the longitudinal tensile load of 118.66 kN, representing the ultimate load at which the FPF occurs. The maximum equivalent stresses at FPF for the rest of the composite laminates are centralised in Table 4.

A comparison between the considered cases is realised with respect to the stiffness properties, in terms of: longitudinal, transverse, in-plane shear and out-of-plane shear elastic moduli; strength properties, in terms of: ultimate loads at which FPF and LPF occurs, and total cost of the laminates, as shown in Figure 5.

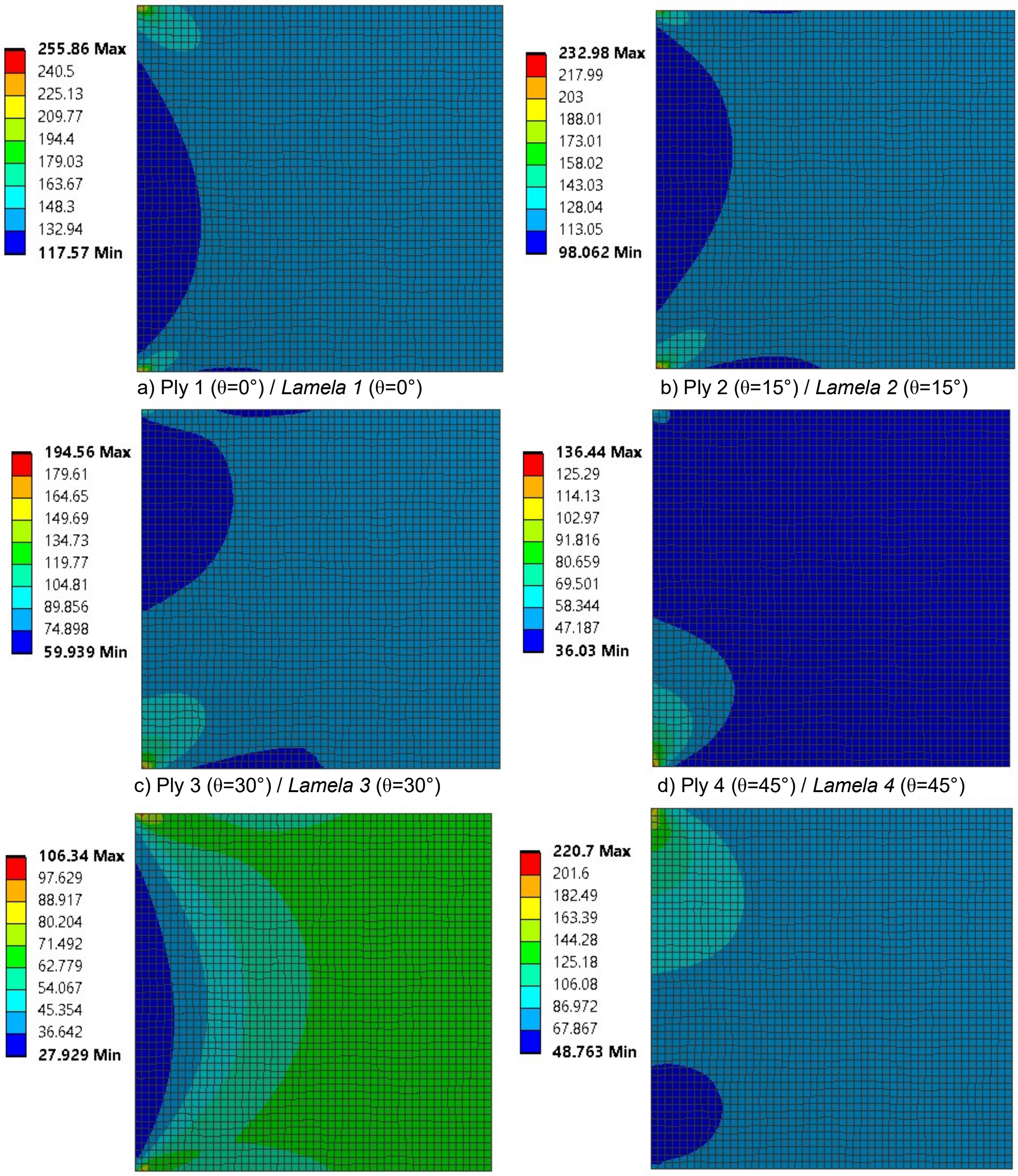

a) Ply 1 (θ=0°) / *Lamela 1* (θ=0°)

b) Ply 2 (θ=15°) / *Lamela 2* (θ=15°)

c) Ply 3 (θ=30°) / *Lamela 3* (θ=30°)

d) Ply 4 (θ=45°) / *Lamela 4* (θ=45°)

e) Ply 5 (θ=90°) / *Lamela 5* (θ=90°)

f) Ply 6 (θ=-45°) / *Lamela 6* (θ=-45°)

Fig. 4 - Stress distribution on ply set for *Case I* – S glass_epoxy laminate / *Distribuția tensiunilor pe straturile stratificatului realizat din fibre de sticlă S și matrice epoxidică (Cazul I).*

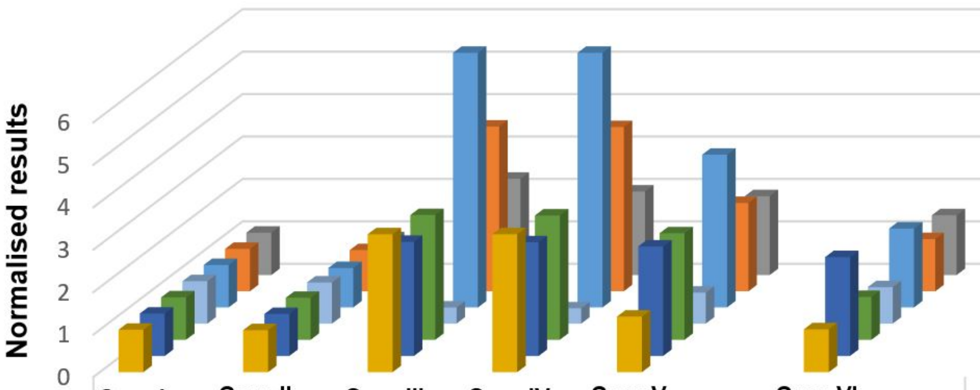

	Case I	Case II	Case III	Case IV	Case V	Case VI
Ex	1	0.99	3.25	3.25	1.31	1.01
Ey	1	0.99	2.69	2.68	2.58	2.33
Gxy	1	0.99	2.94	2.93	2.51	1.01
Gyz	1	0.97	0.38	0.36	0.73	0.86
Price	1	0.93	6.19	6.12	3.6	1.86
Ultimate load FPF	1	0.97	3.88	3.87	2.08	1.23
Ultimate load LPF	1	0.87	2.27	1.97	1.86	1.41

Fig. 5- Comparison between the analysed properties of composite laminates / *Comparație între proprietăţile analizate ale stratificatelor compozite.*

Table 5

The loading steps selected for damage investigation / *Treptele de încărcare selectate pentru investigarea degradărilor*

Loading steps / *Trepte de încărcare*	Tensile loads / *Forțe de tracțiune* [kN]			
	Case I	Case III	Case V	Case VI
1	300	500	350	350
2	350	700	500	450
3	-	-	-	500

5.3. Progressive damage investigations

Progressive damage refers to the local failures that occur in the layers of the laminates when the first ply failure is initiated; the process continues until the composite laminas cannot sustain any additional load [19-22].

In order to investigate the damage initiation and damage propagation in the layers of the balanced laminates, different loading steps are considered, as shown in Table 5, depending on the ultimate loads of each case.

Figures 6-14 give indications about the location of the damage initiations and propagations on the layers of each analysed case presented in Table 5.

The damage status is expressed based on the damage indices, when *0* means undamaged, *1* represents a partial damage and *2* refers to a completely damage [3].

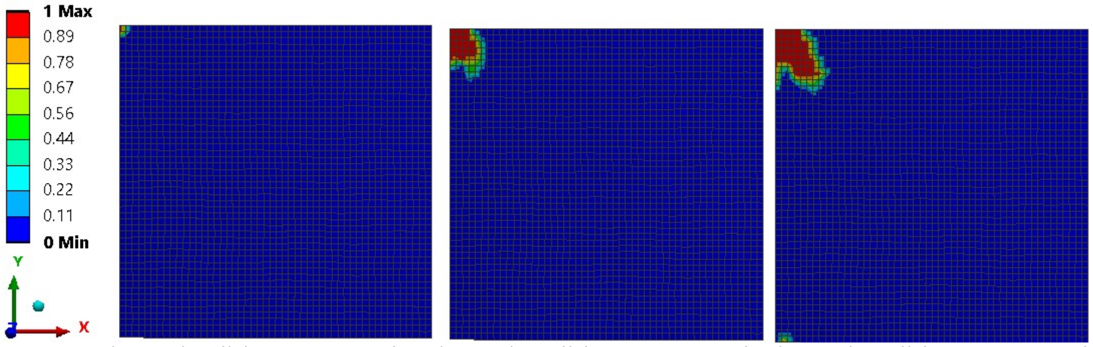

a) Ply 1 (θ=0°) / *Lamela 1 (θ=0°)* b) Ply 2 (θ=15°) / *Lamela 2 (θ=15°)* c) Ply 3 (θ=30°) / *Lamela 3 (θ=30°)*

Fig. 6 continues on next page

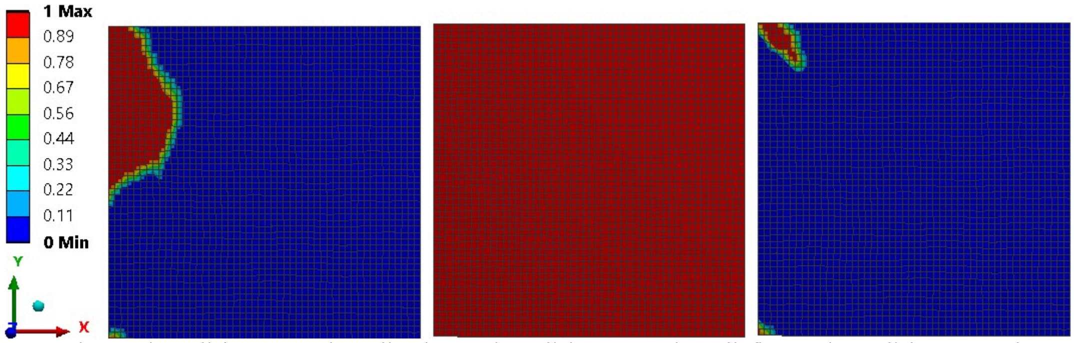

d) Ply 4 (θ=45°) / *Lamela 4* (θ=45°) e) Ply 5 (θ=90°) / *Lamela 5* (θ=90°) f) Ply 6 (θ=-45°) / *Lamela 6* (θ=-45°)

Fig. 6 - Damage location on the layers of *Case I* laminate (S glass_epoxy) at 300 kN tensile load / *Localizarea degradărilor pe straturile stratificatului realizat din fibre de sticlă S și matrice epoxidică (Cazul I) la o tracţiune de 300 kN.*

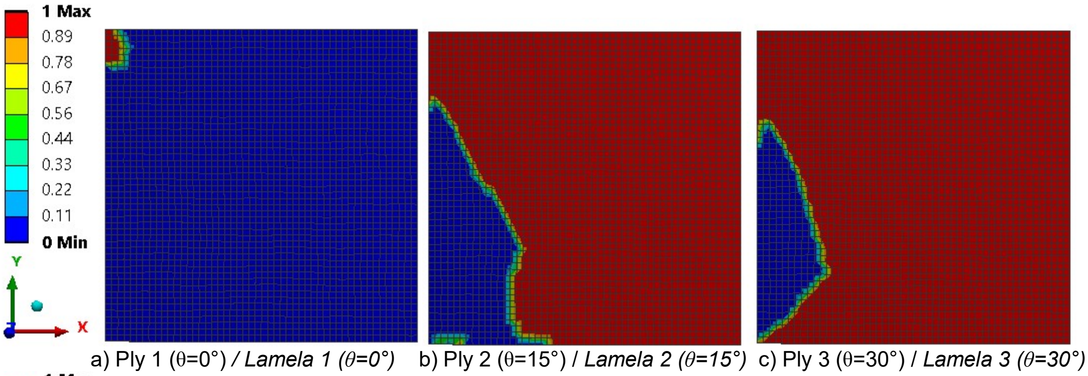

a) Ply 1 (θ=0°) / *Lamela 1 (θ=0°)* b) Ply 2 (θ=15°) / *Lamela 2 (θ=15°)* c) Ply 3 (θ=30°) / *Lamela 3 (θ=30°)*

d) Ply 4 (θ=45°) / *Lamela 4* (θ=45°) e) Ply 5 (θ=90°) / *Lamela 5* (θ=90°) f) Ply 6 (θ=-45°) / *Lamela 6* (θ=-45°)

Fig. 7- Damage evolution on the layers of *Case I* laminate (S glass_epoxy) at 350 kN tensile load / *Localizarea degradărilor pe straturile stratificatului realizat din fibre de sticlă S și matrice epoxidică (Cazul I) la o tracţiune de 350 kN.*

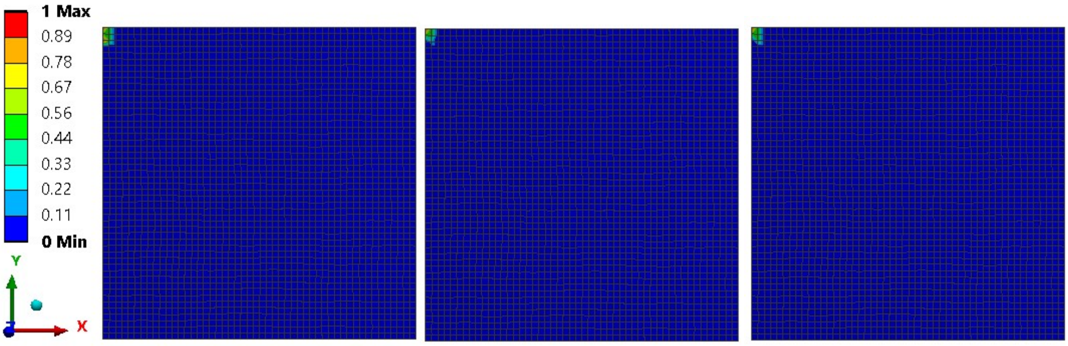

a) Ply 1 (θ=0°) / *Lamela 1* (θ=0°) b) Ply 2 (θ=15°) / *Lamela 2* (θ=15°) c) Ply 3 (θ=30°) / *Lamela 3* (θ=30°)

Fig. 8 continues on next page

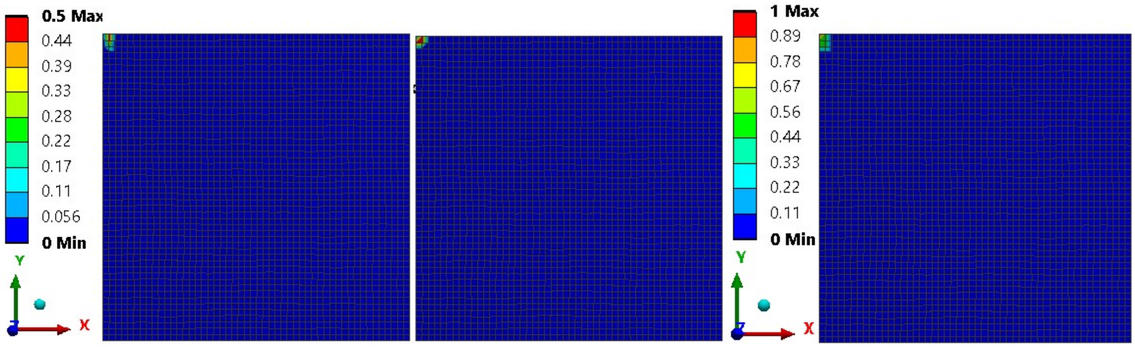

d) Ply 4 (θ=45°) / *Lamela 4* (θ=45°) e) Ply 5 (θ=90°) / *Lamela 5* (θ=90°) f) Ply 6 (θ=-45°) / *Lamela 6* (θ=-45°)

Fig. 8 - Damage location on the layers of *Case III* laminate (carbon_epoxy) at 500 kN tensile load / *Localizarea degradărilor pe straturile stratificatului realizat din fibre de carbon și matrice epoxidică (Cazul III) la o tracţiune de 500 kN.*

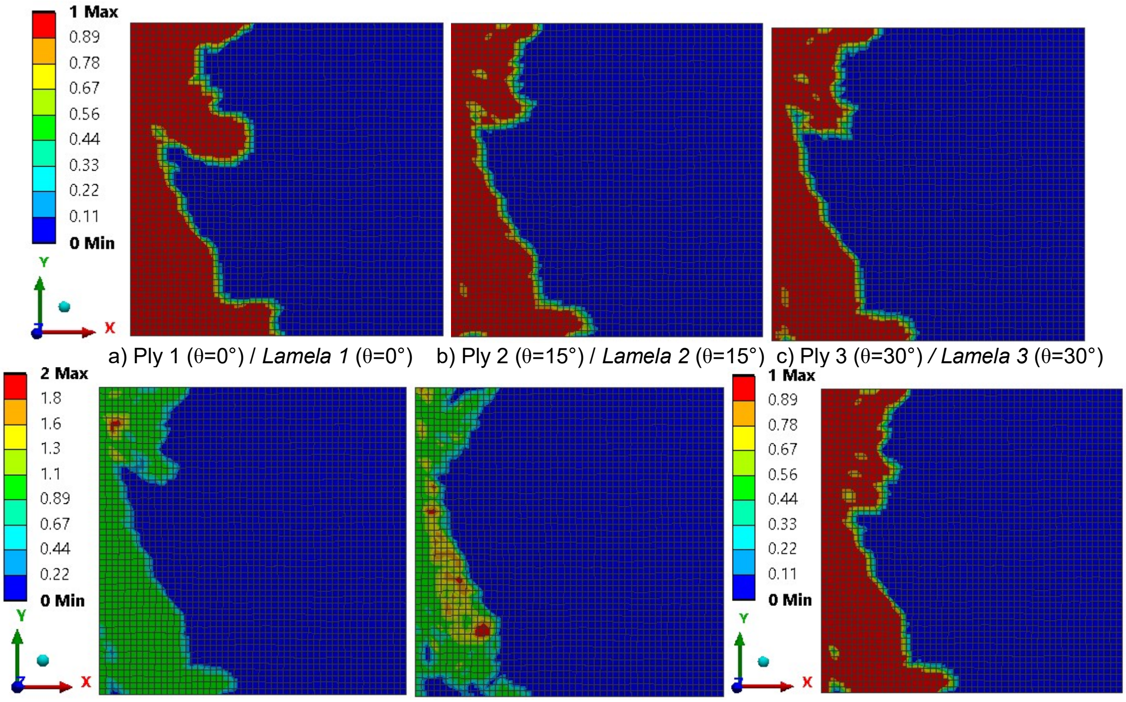

a) Ply 1 (θ=0°) / *Lamela 1* (θ=0°) b) Ply 2 (θ=15°) / *Lamela 2* (θ=15°) c) Ply 3 (θ=30°) / *Lamela 3* (θ=30°)

d) Ply 4 (θ=45°) / *Lamela 4* (θ=45°) e) Ply 5 (θ=90°) / *Lamela 5* (θ=90°) f) Ply 6 (θ=-45°) / *Lamela 6* (θ=-45°)

Fig. 9 - Damage evolution on the layers of *Case III* laminate (carbon_epoxy) at 700 kN tensile load / *Localizarea degradărilor pe straturile stratificatului realizat din fibre de carbon și matrice epoxidică (Cazul III) la o tracţiune de 700 kN.*

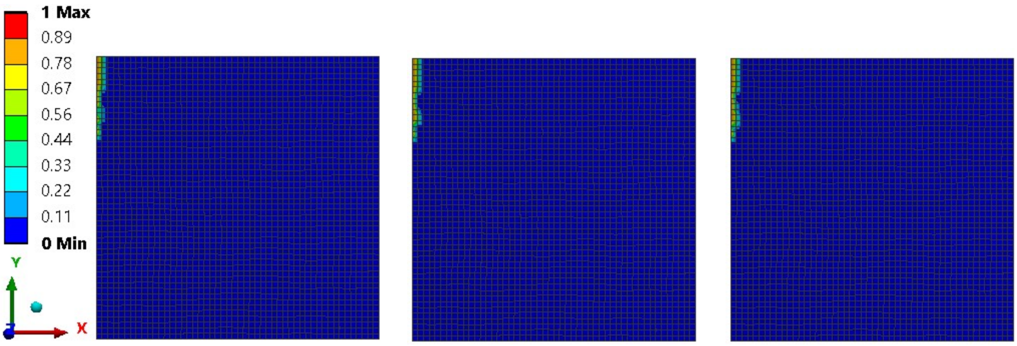

a) Ply 1 (θ=0°) / *Lamela 1* (θ=0°) b) Ply 2 (θ=15°) / *Lamela 2* (θ=15°) c) Ply 3 (θ=30°) / *Lamela 3* (θ=30°)

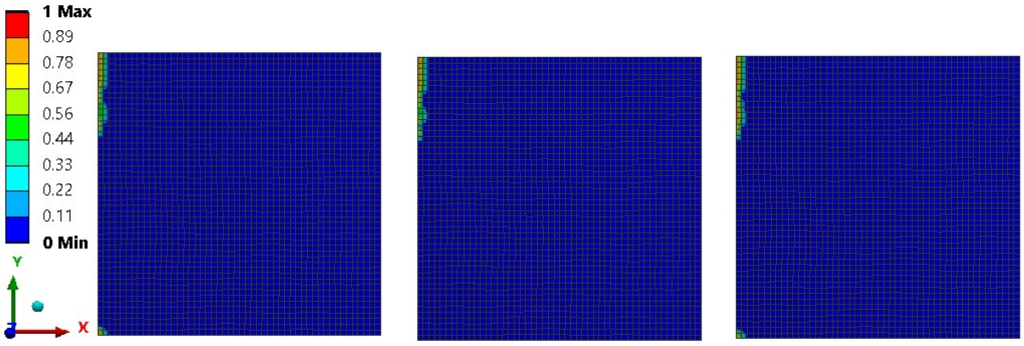

d) Ply 4 (θ=45°) / *Lamela 4* (θ=45°) e) Ply 5 (θ=90°) / *Lamela 5* (θ=90°) f) Ply 6 (θ=-45°) / *Lamela 6* (θ=-45°)

Fig. 10 - Damage evolution on the layers of *Case V* hybrid laminate at 350 kN tensile load / *Localizarea degradărilor pe straturile stratificatului hibrid (Cazul V) la o tracţiune de 350 kN.*

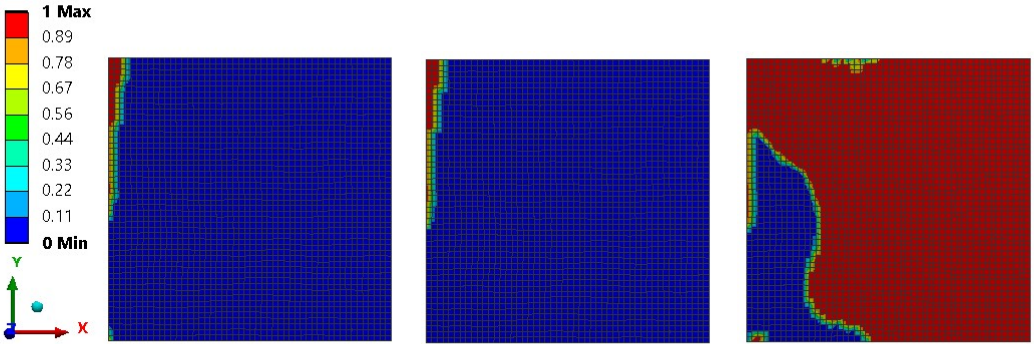

a) Ply 1 (θ=0°) / *Lamela 1* (θ=0°) b) Ply 2 (θ=15°) / *Lamela 2* (θ=15°) c) Ply 3 (θ=30°) / *Lamela 3* (θ=30°)

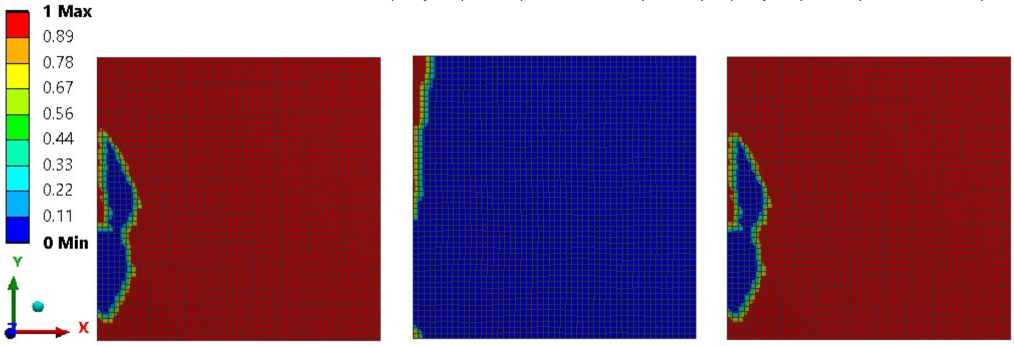

d) Ply 4 (θ=45°) / *Lamela 4* (θ=45°) e) Ply 5 (θ=90°) / *Lamela 5* (θ=90°) f) Ply 6 (θ=-45°) / *Lamela 6* (θ=-45°)

Fig. 11 - Damage evolution on the layers of *Case V* hybrid laminate at 500 kN tensile load / *Localizarea degradărilor pe straturile stratificatului hibrid (Cazul V) la o tracţiune de 500 kN.*

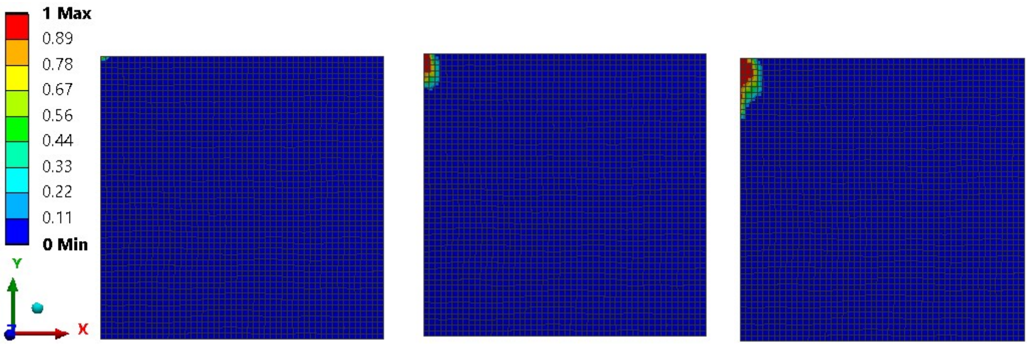

a) Ply 1 (θ=0°) / *Lamela 1* (θ=0°) b) Ply 2 (θ=15°) / *Lamela 2* (θ=15°) c) Ply 3 (θ=30°) / *Lamela 3* (θ=30°)

Fig. 12 continues on next page

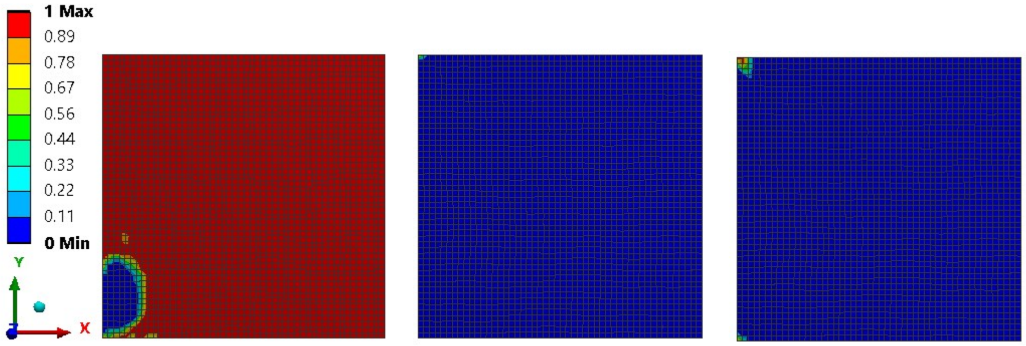

d) Ply 4 (θ=45°) / *Lamela 4* (θ=45°) e) Ply 5 (θ=90°) / *Lamela 5* (θ=90°) f) Ply 6 (θ=-45°) / *Lamela 6* (θ=-45°)

Fig. 12 - Damage evolution on the layers of *Case VI* hybrid laminate at 350 kN tensile load / *Localizarea degradărilor pe straturile stratificatului hibrid (Cazul VI) la o tracţiune de 350 kN.*

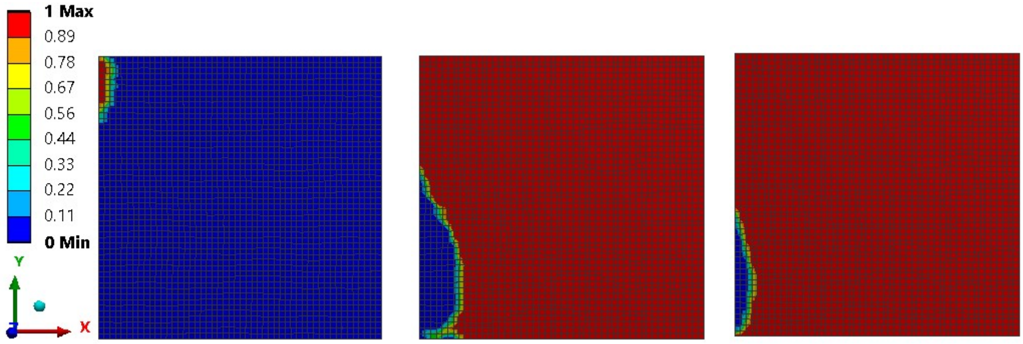

a) Ply 1 (θ=0°) / *Lamela 1* (θ=0°) b) Ply 2 (θ=15°) / *Lamela 2* (θ=15°) c) Ply 3 (θ=30°) / *Lamela 3* (θ=30°)

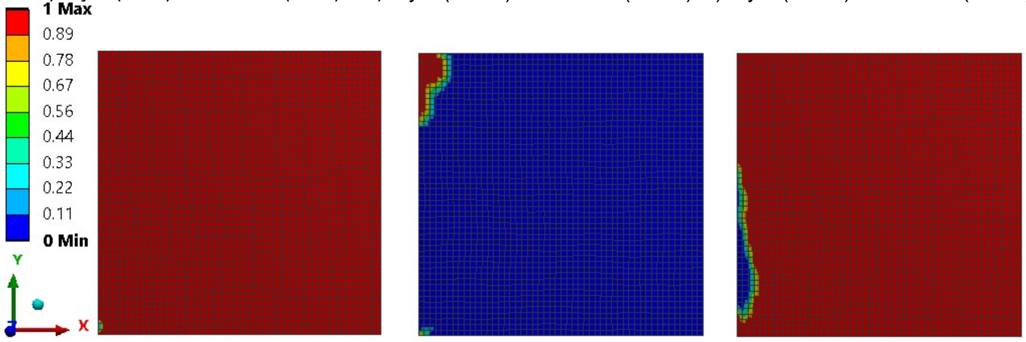

d) Ply 4 (θ=45°) / *Lamela 4* (θ=45°) e) Ply 5 (θ=90°) / *Lamela 5* (θ=90°) f) Ply 6 (θ=-45°) / *Lamela 6* (θ=-45°)

Fig. 13 - Damage evolution on the layers of Case VI hybrid laminate at 450 kN tensile load / *Localizarea degradărilor pe straturile stratificatului hibrid (Cazul VI) la o tracţiune de 450 kN.*

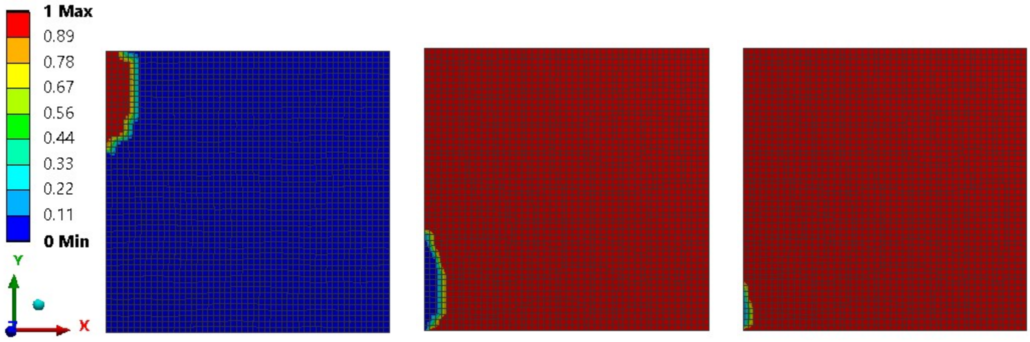

a) Ply 1 (θ=0°) / *Lamela 1* (θ=0°) b) Ply 2 (θ=15°) / *Lamela 2* (θ=15°) c) Ply 3 (θ=30°) / *Lamela 3* (θ=30°)

Fig. 14 continues on next page

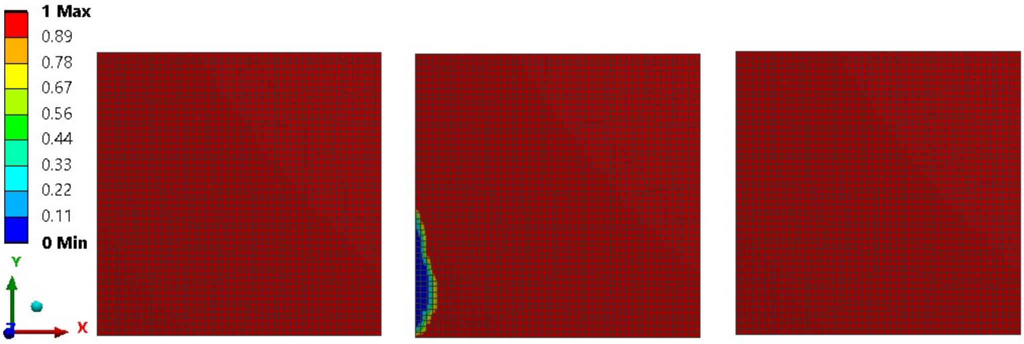

d) Ply 4 (θ=45°) / *Lamela 4* (θ=45°) e) Ply 5 (θ=90°) / *Lamela 5* (θ=90°) f) Ply 6 (θ=-45°) / *Lamela 6* (θ=-45°)

Fig. 14 - Damage evolution on the layers of *Case VI* hybrid laminate at 500 kN tensile load / *Localizarea degradărilor pe straturile stratificatului hibrid (Cazul VI) la o tracţiune de 500 kN.*

The sequence of the plies failure can be pointed out and the progressive damages of composite laminates can be concluded for different loading steps as shown in Figures 6-14.

The damage propagations in the layers of the composite laminates occur with the following sequences: *Case I* and *Case III* – 90°, 45°, 30°, -45°, 15°, 0°; *Case* V – -45°, 45°, 30°, 15°, 90°, 0° and *Case VI* – 45°, 30°, -45°, 15°, 90°, 0°.

The gradual failure of hybrid I laminate is achieved due to the balanced behaviour of fibres orientations and because of the adopted composite material and its stacking sequence. Figure 11 shows that at a tensile load of 500 kN, significant damages occur in only 3 laminas.

6. Conclusions

A comparative analysis has been carried out, for 6 different composite material laminates and same fibres orientations configuration, in terms of in-plane and flexural engineering constants, total cost, ultimate loads at FPF and LPF, and their corresponding equivalent stresses on the layers of the multi-layered element. Moreover, the initiation and evolution of damages on the laminas of the multi-layered plates have been illustrated and the sequences of the plies failure of the laminates have been established.

Although the carbon fibres reinforced multi-layered elements have improved stiffness and strength properties, the total price is 6 times higher than the S glass fibres laminates. Therefore, the studied hybrid laminates can be considered as feasible solutions, since the stiffness and strength characteristics are increased compared to the *Case I* and *Case II* and the cost is lower than the carbon fibres reinforced multi-layered plates.

REFERENCES

1. I.M. Daniel, O. Ishai, Engineering Mechanics of Composite Materials. Second Edition, Oxford Univ. Press, Oxford, New York, 2006.
2. I. Hudișteanu, N. Ţăranu, I-S. Enţuc, S.G. Maxineasa, Comparative Analysis of the engineering constants of composite laminates, Rev Rom Mat, 2016, **46**(2), 232.
3. ANSYS® Documentation, ANSYS, Inc.
4. D.J. Mortell, D.A. Tanner, C.T. McCarthy, An experimental investigation into multi-scale damage progression in laminated composites in bending, Compos Struct, 2016, **149**, 33.
5. B.B. Liao, P.F. Liu, Finite element analysis of dynamic progressive failure of plastic composite laminates under low velocity impact, Compos Struct, 2017, **159**, 567.
6. N. Ţăranu, D. Banu, G. Oprișan, M. Budescu, L. Bejan, Strengthening of thin reinforced concrete slabs with composite strips, Rev Rom Mat, 2013, **43**(1), 3.
7. M. Sonmez, D. Ficai, A. Ficai, L. Alexandrescu, G. Voicu, E. Andronescu, Functionalization of glass fibers for obtaining polypropylene based composite materials, Romanian Journal of Materials, 2014, **44**(1), 88.
8. G. Oprișan, N. Ţăranu, M. Budescu, I. Enţuc, Structural behaviour of reinforced concrete beams strengthened by CFRP plate bonding, Romanian Journal of Materials, 2012, **42**(4), 387.
9. M. Dima, C. Frâncu, Method for testing glass fibre reinforced polymer composites (GFRP's) with polyester matrix, Romanian Journal of Materials, 2014, **44**(3), 304.
10. L. Bejan, A. Sîrbu, N. Ţăranu, Component properties influence upon the elasticity modules of cloth-reinforced polymeric composites, Materiale Plastice, 2007, 44(1), 22.
11. L. Bejan, N. Ţăranu, A. Sârbu, Advanced polymeric composites with hybrid reinforcement, J Optoelectron Adv M, 2010, **12**(9), 1930.
12. www.easycomposites.co.uk
13. N. Ţăranu, L. Bejan, R. Cozmanciuc, R. Hohan, Elements of composite materials, Politehnium Publishing House, Iaşi, 2013.
14. E.J. Barbero, Introduction to Composite Materials Design. Second Edition, CRC Press, Taylor & Francis Group, New York, 2011.
15. R.M. Jones, Mechanics of Composite Materials. Second Edition, Taylor & Francis, Inc., Philadelphia, 1999.
16. A.K. Kaw, Mechanics of composite materials, Second edition, CRC Press, Taylor & Francis, Boca Raton, 2006.
17. R.F. Gibson, Principles of Composite Material Mechanics, CRP Press, Taylor & Francis Group, Boca Raton, 2012.
18. C.T. Herakovich, Mechanics of Fibrous Composites, John Wiley & Sons, Inc., Univ. of Virginia, United States of America, 1998.
19. N.K. Parambil, S. Gururaja, Micromechanical damage analysis in laminated composites with randomly distributed fibers, J Compos Mater, 2016, **50** (21), 2911.
20. B. Hongchen, L. Guangyan, Progressive failure analysis on scaled open-hole tensile composite laminates, Compos Struct, 2016, **150**, 173.
21. G. Zhangxin, Z. Hao, L. Yongcun, H. Xiaoping, W. Zhihua, Simulating Initial and Progressive Failure of Open-Hole Composite Laminates under Tension, Appl Compos Mater, 2016, **23**, 1209.
22. E.J. Pineda, B.A. Bednarcyk, S.M. Arnold, Validated progressive damage analysis of simple polymer matrix composite laminates exhibiting matrix microdamage: Comparing macromechanics and micromechanics, Compos Sci Technol, 2016, **133**, 184.

****